

Two-dimensional Numerical Simulation of Combustion and Heat Transfer in Porous Burners

Meisam Farzaneh, Reza Ebrahimi, Mehrzad Shams, and Mohammad Shafiey

Abstract—In this study, combustion in a 5kW porous burner is simulated. The two dimensional Navier-Stokes, the energy and the chemical species transport equations are solved and a multistep kinetics mechanism (5 reactions and 7 species) is employed. Finite volume method is used for simulation. Thermal nonequilibrium is accounted for gas and solid temperature and radiation heat transfer is considered for solid phase. Gas and solid temperature profiles and species mole fractions on the burner centerline are presented. Calculated CO and NO emissions are compared to experimental data for several excess air ratios. The effects of excess air ratio and solid phase radiation are investigated. The predicted temperature profile and pollutants formation are in good agreement with the available experimental data.

Index Terms— Combustion, numerical study, Porous burner, two dimensional

I. INTRODUCTION

The interest in combustion of hydrocarbon fuels within porous media has increased significantly during recent years. This technology combines higher power densities, high efficiencies, higher power dynamic ranges and very low emissions of pollutants (NO_x , CO). In porous burner, the porous matrix recirculates heat from the postflame to the preflame zone through solid to solid radiation and conduction. Weinberg [1] is one of the first researchers introduced the idea of excess enthalpy burners through a theoretical analysis. He presented the idea of using a heat exchanger to recirculate heat as opposed to recirculation hot products in to the reactants, which results in a dilution of the reactants. The concept of using porous media in the radiation zone of a premixed flame to obtain internal heat recirculation was introduced by Takeno, Sato and Hase [2]. They showed theoretically that by transferring energy from the exhaust gas to the unburnt mixture, the flame temperature and flame speeds were

significantly increased. After that many experiments were performed on porous ceramic burners [3]-[4]-[5]. A very comprehensive review of the different states of combustion in porous media has been presented in [6].

The reduction in time between a system concept and commercialization and the increase in the cost of testing will demand a greater reliance on numerical models to simulate the systems and reduce the cost and time to develop a product. Thus, much research has been dedicated to the numerical modeling of heat transfer and combustion with varying degrees of accuracy. Hsu, Howell, and Matthews [7] developed a numerical model of a porous ceramic burner which included multistep chemistry. Their results also showed an increased flame speed and an extension of the lean limit to 0.33 which is in qualitative agreement with the experimental observation. Zhou and Preira [8] assumed one dimensional combustion in a porous burner. They considered detailed reaction mechanism of methane-air combustion, (27 species and 73 reactions), convective heat transfer of solid-gas and radiative heat transfer in the porous media. They presented a numerical study which showed the effects of excess air ratio thermal power, solid conductivity and radiative heat transfer on the combustion and pollutants formation in porous media.

Diamantis, Mastorakos, and Goussis [9] developed a mathematical model for combustion in porous media for both surface and submerged flames over a wide range of operation condition. Their model success was attributed to the detailed given to boundary conditions and the radiation modeling, which was done by solving the radiation transfer equation inside the porous media without any simplifying. The model reproduced experimental data for both single and two layer surface flame.

Smucker and Ellzey [10] studied a two section porous burner through experiments and computations. In the experimental study the stable operating range with propane-air and methane-air mixtures was investigated. The burner included 23.6 PPC upstream sections and 3.9 PPC down stream section, each made from YZA ceramic foam.

In the present study the behavior of methane-air combustion in a conical porous burner numerically investigates. The Navier-Stokes, the energy and the chemical species transport equations are solved in a two dimensional axisymmetric model. In order to predict CO and NO emissions, Multistep chemical kinetics is applied, which consists of 5 reactions and 7 species. Predicted centerline gas and solid temperature are compared with available experimental data. The effects of excess air ratio on flame behavior and pollutants formation are investigated

M. Farzaneh is with the Department of Mechanical Engineering, K. N. Toosi University of Technology, Tehran, 1656983911 Iran (e-mail: meisamfarzaneh@gmail.com).

R. Ebrahimi is with the Department of Aerospace Engineering, K. N. Toosi University of Technology, Tehran, 1656983911 Iran (e-mail: rezaeb@yahoo.com).

M. Shams is with the Department of Mechanical Engineering, K. N. Toosi University of Technology, Tehran, 1656983911 Iran (e-mail: shams@kntu.ac.ir).

M. shafiey is with the Department of Mechanical Engineering, K. N. Toosi University of Technology, Tehran, 1656983911 Iran (e-mail: Shafiey.Mohammad@gmail.com).

and compared with experiments. Also, the influence of radiative heat transfer on final results is assessed.

II. POROUS BURNER GEOMETRY

The burner which was made and tested at LSTM-University of Erlangen-Nuremberg [11] is used in this simulation. This 10kW burner-heat exchanger system is divided into three regions. The preheating zone consists of 3 and 5 mm alumina spheres; the combustion zone is made of 10PPI SiC ceramic foam and heat exchanger zone which is filled with 3 and 5 mm alumina spheres. The internal diameters of preheating and combustion regions are respectively 40 and 74 mm and the total length of the porous burner is 260 mm. The burner walls are water cooled, but the combustion region is insulated from the cold walls by ceramic insulation. A sketch of porous burner is shown in Fig. 1.

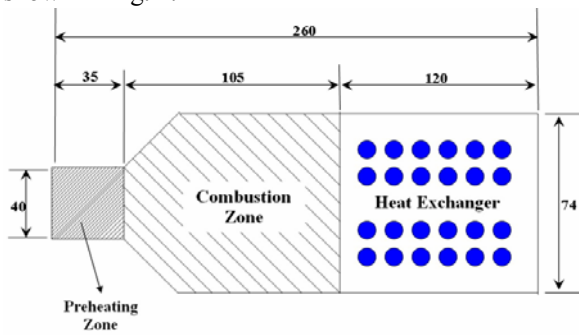


Fig. 1. Porous medium burner with heat exchanger

III. MATHEMATICAL SIMULATION

Two-dimensional axisymmetric geometry, steady, laminar and Newtonian flow, inert homogeneous porous material with negligible catalytic effects is assumed. In Combustion modeling multistep kinetics are considered, which consists of 5 reactions and 7 chemical species [12]. Under these assumptions, the governing equations are given below.

A. Continuity Equation

$$\nabla \cdot (\rho V) = 0 \quad (1)$$

B. Axial Momentum Equation

$$\nabla \cdot (\rho u V) = -\frac{\partial P}{\partial x} + \nabla \cdot (\mu \nabla u) - \left(\frac{\Delta P}{\Delta L} \right)_x \quad (2)$$

C. Radial Momentum Equation

$$\nabla \cdot (\rho v V) = -\frac{\partial P}{\partial r} + \nabla \cdot (\mu \nabla v) - \left(\frac{\Delta P}{\Delta L} \right)_r \quad (3)$$

D. Gas Phase Energy Equation

$$\nabla \cdot (\rho V C_p T_f) = \nabla \cdot (\phi \lambda_f \nabla T_f) + H(T_s - T_f) - \phi \sum_{k=1}^{NS} \dot{\omega}_k h_k W_k \quad (4)$$

E. Solid Phase Energy Equation

$$0 = \nabla \cdot ((1 - \phi) \lambda_s \nabla T_s) + H(T_f - T_s) - \nabla \cdot q \quad (5)$$

Since locally, the solid and gas temperature may be different, separate energy equations for the solid and the gas phases are solved. These two equations were coupled through a convective heat transfer term. The volumetric heat transfer coefficient between gas and solid, for packed bed (preheating and heat exchanger zones) is estimated from the experimental correlation of Wakao and Kaguei [13]:

$$H = \left(\frac{6\phi}{d_p^2} \right) \lambda_f Nu_v ; \quad Nu_v = 2.0 + 1.1 Re^{0.6} Pr^{1/3} \quad (6)$$

and the one of Younis and Viskanta [14] for ceramic foam (combustion zone):

$$H = \left(\frac{\lambda_f}{d_p^2} \right) Nu_c ; \quad Nu_c = 0.146 Re^{0.96} \quad (7)$$

E. Species Conservation Equation

$$\nabla \cdot (\rho V Y_k) = \nabla \cdot (\rho D_{km} \nabla Y_k) + \dot{\omega}_k W_k \quad k \in [1, N_S] \quad (8)$$

The 5-step reduced reaction mechanism for methane oxidation is used to simulate chemical reaction in porous media. This mechanism consists of 7 species which contains CH₄, O₂, N₂, CO₂, H₂O, CO and NO.

Pressure loss due to porous matrix is accounted using [15]:

$$\left(\frac{\Delta P}{\Delta L} \right)_i = 180 \frac{(1 - \phi)^2}{\phi^3} \frac{\mu u_i}{d_p^2} + 1.8 \frac{1 - \phi}{\phi^3} \frac{\rho |V| u_i}{d_p} \quad (9)$$

IV. RADIATION MODELING

Gas radiation is not considered since the solid has a high emissivity when compared to the gas. Emission, absorption and scattering by the porous media are considered. To determine the radiative heat flux, the solid and fluid phases are considered as a single continuum homogeneous phase and the radiative transfer equation is solved. The heat source term $\nabla \cdot q$ due to radiation in solid phase that appears in equation (5) is calculated from equation (10):

$$\nabla \cdot q = \kappa \left(4\pi I_b - \int_{4\pi} I d\Omega \right) \quad (10)$$

Radiative intensity is obtained by solving the radiative transfer equation:

$$\frac{dI(\vec{r}, \hat{s})}{ds} = -(\kappa(\vec{r}) + \sigma_s(\vec{r})) I(\vec{r}, \hat{s}) + S(\vec{r}, \hat{s}) \quad (11)$$

where the source function is:

$$S(\vec{r}, \hat{s}) = \kappa(\vec{r}) I_b(\vec{r}) + \frac{\sigma_s(\vec{r})}{4\pi} \int_{4\pi} I(\vec{r}, \hat{s}') \Phi(\hat{s}', \hat{s}) d\Omega' \quad (12)$$

The radiation intensity $I(\vec{r}, \hat{s})$ is a function of position and direction. The expression on the left-hand side represents the

gradient of the intensity in the specified direction \hat{s} . The first term on the right hand side represents intensity loss due to absorption and outscattering. The two source terms in equation (12) represent intensity gain due to emission and in-scattering. Each porous medium is assumed gray, homogeneous and the scattering isotropic ($\Phi = 1$).

The correlation of the radiative extinction coefficient for the SiC foam, are obtained from [16]. For the packed bed with large diffusely reflecting spheres assumption, the scattering and absorption coefficients are calculated by [17].

V. BOUNDARY CONDITION

The following boundary conditions are used:

A. At the inlet

$$u = u_{in}; v = 0; T_f = T_{f,in}; (1 - \phi)\lambda_s \frac{\partial T_s}{\partial x} = -\varepsilon_r \sigma (T_s^4 - T_0^4) \quad (13)$$

$$; I = \frac{\sigma T_s^4}{\pi}; Y_k = Y_{k,in}, \quad k = 1, 2, \dots, 7$$

B. At the outlet

$$\frac{\partial u}{\partial x} = \frac{\partial v}{\partial x} = \frac{\partial T_f}{\partial x} = \frac{\partial Y_{k,in}}{\partial x} = 0, \quad k = 1, 2, \dots, 7; \quad (14)$$

$$(1 - \phi)\lambda_s \frac{\partial T_s}{\partial x} = -\varepsilon_r \sigma (T_s^4 - T_0^4); I = \frac{\sigma T_s^4}{\pi}$$

C. At the axis symmetric condition are imposed

$$v = \frac{\partial u}{\partial x} = \frac{\partial T_f}{\partial x} = \frac{\partial T_s}{\partial x} = \frac{\partial Y_k}{\partial x} = 0 \quad (15)$$

At the burner wall and tube surfaces, no-slip and impenetrability condition are applied to the momentum equations, and the gradient of the mass fraction and normal to the surface is set zero. These surfaces are considered gray, emitting and reflecting diffusely; therefore, the boundary intensity for outgoing direction is:

$$I(\vec{r}) = \varepsilon I_b(\vec{r}) + \frac{1 - \varepsilon}{\pi} \int_{\hat{s} \cdot n < 0} I(\vec{r}, \hat{s}) |\hat{s} \cdot n| d\Omega \quad (16)$$

At the tube surface, the boundary condition for the energy equation involves a specification of the heat flux to the tube walls. The heat flux is computed from the expression:

$$q = - \left(\lambda_s \frac{\partial T_s}{\partial n} + \lambda_f \frac{\partial T_f}{\partial n} \right) \quad (17)$$

where n is the outward normal to the tube surface, T_C is the temperature of the coolant within the tube, and R_t is the total thermal resistance between the bed and the coolant:

$$R_t = \frac{1}{h} + \frac{r_i \ln(r_o / r_i)}{\lambda_{tube}} + R_{contact} \quad (18)$$

VI. NUMERICAL PROCEDURE

For the spatial discretization of governing equations, a finite volume method is employed in an axisymmetric cylindrical

geometry. The solution domain is discretized by a structured mesh of quadrilateral elements. Typical distances between grid points lay between 0.5 mm. Pressure and velocity are coupled by the SIMPLE algorithm [18]. Radiative transport equation is solved by standard finite volume method [19]. Since the finite volume method is a popular approach for fluid flow and heat transfer, it is desirable to use a radiation transport procedure that shares the same computational grid with the finite volume method. The same computational grid is used for convenience, because it eliminates the need to interpolate temperature and other physical properties and allows use of the same linear equation solvers. For all the equations a relative convergence of 10^{-6} is specified.

VII. RESULTS

At the present work, combustion of methane/air fuel in the three-region porous burner is studied for different conditions. The effect of excess air ratio is studied on the temperature profiles and emission of CO and NO. The importance of radiative heat transfer of solid phase is investigated on the flame front. Also, the numerical results are compared with available experimental data.

Figs. 2 and 3 show the comparison between predicted and experimental centerline gas and solid temperatures for a power of 5 kW and excess air ratios of 1.5 and 1.6, respectively. The experimental results have been obtained by Durst and Trimis [20]. Since nonequilibrium assumption is considered for solid and gas energy equations, their temperatures are different in both preheating and combustion zones. As expected, the gas temperature in combustion zone is higher than the solid temperature and the solid phase transfer generated heat to preheating zone through radiation and conduction.

Flame front is formed in conic part of combustion zone and calculated flame front location (0.05 m and 0.06 m from the inlet for excess air ratio of 1.5 and 1.6, respectively) is in good agreement with experimental data. Numerical peak temperature is higher than experimental results and in combustion zone numerical results are slightly different with experimental data. As seen from these two figures, with increasing the excess air ratio, the velocity of gas/air mixture and the flow rate increase. Consequently the porous material in the upstream region (PR) is better cooled and causes the flame front to move downstream and the peak temperature to decrease.

The difference between numerical solutions and experiments can be attributed to some parameters such as solid conductivity, radiative properties and the heat transfer coefficient between solid and gas. Any perturbation in these parameters changes the final results significantly. These parameters are specified by experimental works; Because of porous medium complicated structure, different manufacturers, determination of heat transfer coefficients are very difficult and uncertain.

In Fig. 4 the predicted centerline species mole fraction in the near the flame front are presented. Fig. 5 shows temperature profile and CO profile within the porous medium. Since the CH₄ is almost completely consumed at flame front, the concentration of the CO reaches its maximum near the flame

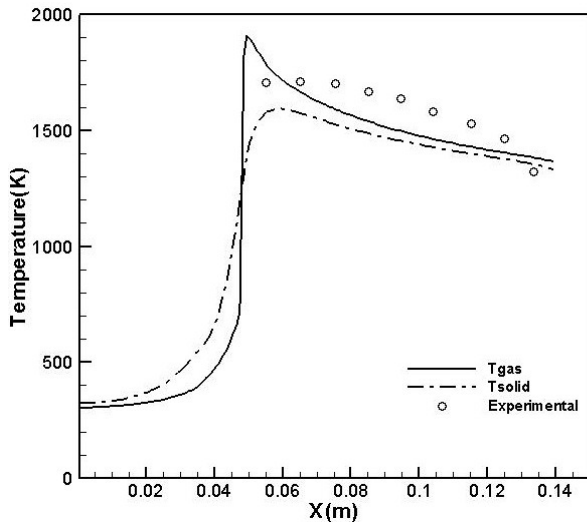


Fig. 2. Comparison of calculated and experimental centerline temperature profiles for excess air 1.5, power 5kW

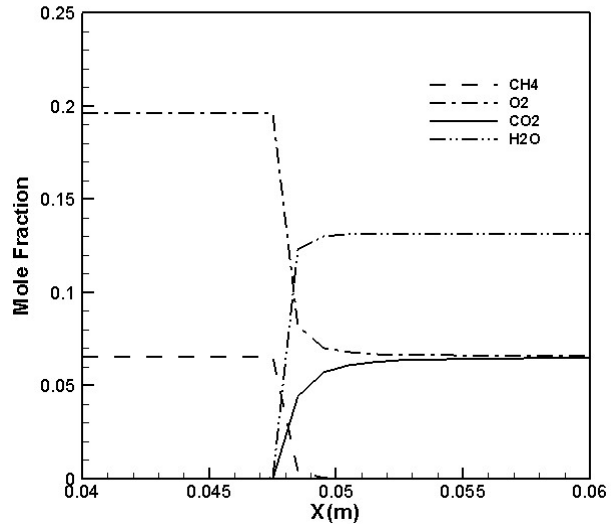


Fig. 4. Centerline species mole fraction near the flame front, for a 5 kW power and an excess air ratio of 1.5

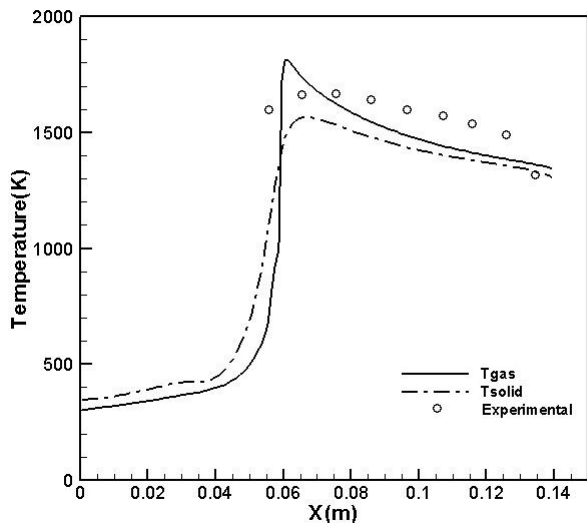


Fig. 3. Comparison of calculated and experimental centerline temperature profiles for excess air 1.6, power 5kW

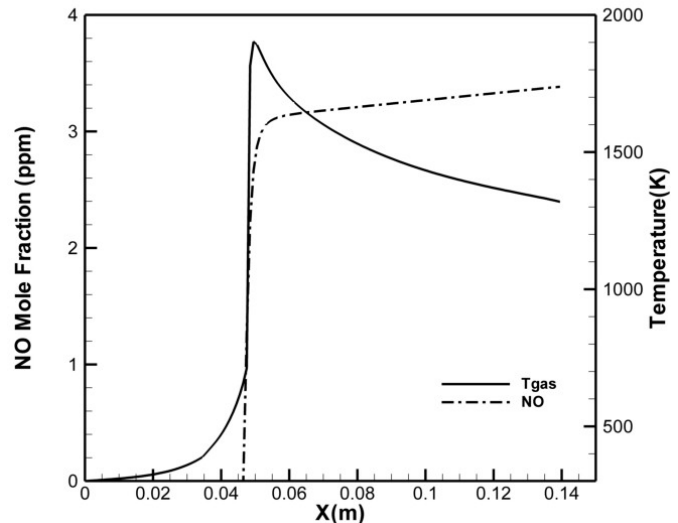


Fig. 5. Temperature and NO profiles as a function of axial distance, for a 5 kW power and an excess air ratio of 1.5

front but afterwards oxidizes slowly and converted to CO_2 further downstream. The NO formation is significantly affected by the flame temperature. As seen in Fig. 6 most of the NO is produced at the flame front.

The excess air ratio effects are studied on the CO and NO emissions. Fig. 7 displays the calculated results of NO mass fraction at the exit for excess air ratios from 1.2 to 1.6 and power 5 kW. The excess air ratio has a significant effect on the emission of NO. The NO concentration decreases with the increase of the excess air ratio. NO can be produced by the thermal mechanism and the prompt mechanism. Both mechanisms are temperature dependent, lower temperatures resulting in lower NO levels. Therefore, the formation of NO depends mainly on the maximum temperatures of the combustion region and on the residence time in the hot region. By increasing the excess air ratio at the same power, the velocity and the gas/air mixture flow rate increases. Consequently, the solid and gas temperatures decrease in the

upstream region and causes the peak temperature to decrease. Thus, the NO emissions are higher for lower excess air ratios. The predictions are in good agreement with the experiments.

Also, the CO emissions are compared with experimental data. As seen from the Fig. 8, the excess air ratio has a significant role on CO emissions. For the power 5kW, the CO emissions decrease from 26 ppm to 10 ppm in range of 1.2 and 1.6 excess air ratios. But minimum CO emissions are obtained in 1.5 excess air ratio. The predictions present the same trend as the experiments.

The base temperature predictions are compared with the temperatures calculated neglecting radiation. The importance of radiation in the temperature profiles can be seen in Fig. 6, where the centerline temperatures obtained considering radiation are compared with the prediction obtained neglecting it. Because of the low temperature in preheating zone, radiation term does not affect the temperature profiles in this region. But in high temperature combustion zone this effects are significant. The

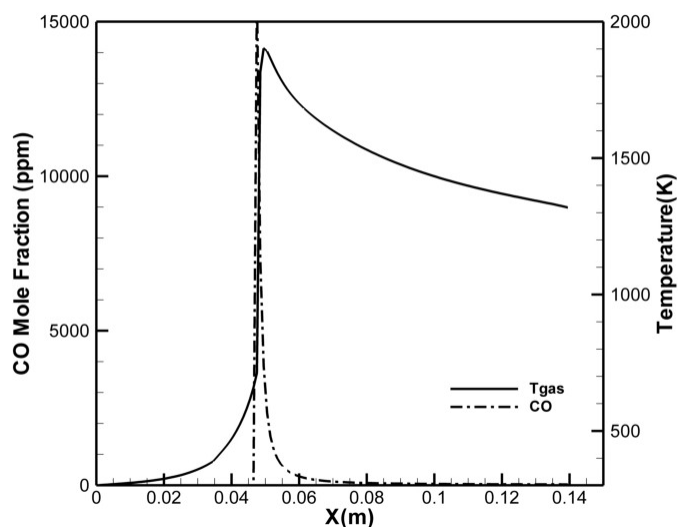


Fig. 6. Temperature and NO profiles as a function of axial distance, for a 5 kW power and an excess air ratio of 1.5

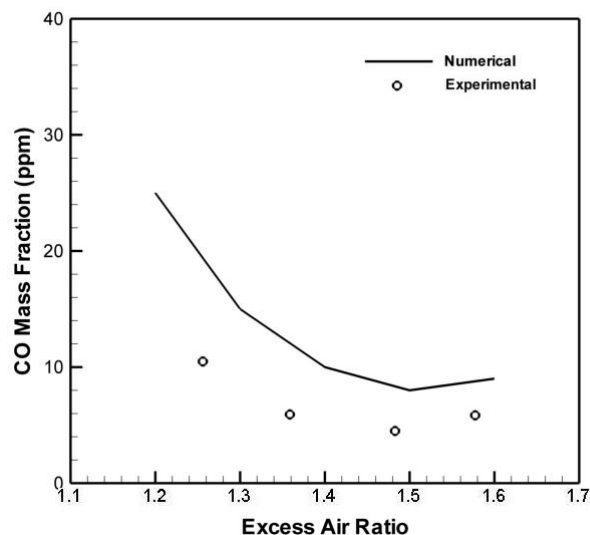


Fig. 8. Comparison of numerical solutions with experiments for emission of CO, power 5 kW

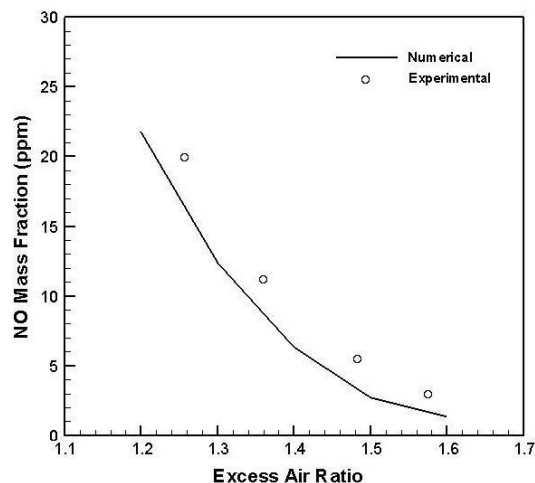


Fig. 7. Comparison of numerical solutions with experiments for emission of NO, power 5 kW

maximum temperature difference occurred in the postflame region. The predictions differ considerably; the ones obtained with radiation are much closer to the experimental data. This supports the claim that, for this particular case of porous burners, radiative heat transfer should be considered and that, by neglecting it, the numerical predictions may be very different from the reality.

VIII. CONCLUSION

Numerical prediction of flow, heat transfer and combustion in porous media are investigated. The combustion reaction is modeled by the multistep reaction mechanism which consists of 5 reactions and 7 species. The effects of excess air ratio on the temperature profiles and pollutants emissions are studied. The flame front location and pollutants are influenced by excess air ratio. By increasing the excess air ratio in the same power, flame front moves downstream, peak temperature decreases and both NO and CO emissions are decreased. For the isotropic media,

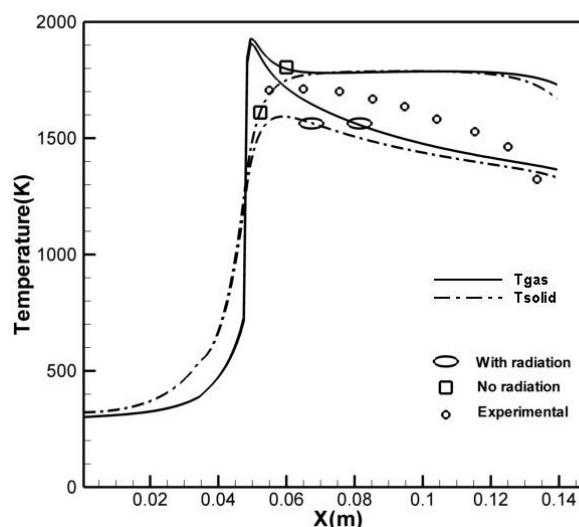


Fig. 9. Comparison of numerical solutions with experimental centerline gas temperature profiles for a 5kW power and a 1.5 excess air ratio coefficient. The results are obtained both considering and neglecting solid phase radiation.

radiative heat transfer equation is solved by finite volume method and importance of solid phase radiation on the temperature profiles is numerically assessed. Temperature profile without consideration of solid phase radiation has large difference with the experiments. The numerical model in this study sufficiently predicts the combustion and pollutants emissions in the experimental porous medium.

ACKNOWLEDGMENT

This work is supported in part by the Research, Development, and Technology Affairs of National Iranian Gas Company (NIGC). The authors extend their appreciation for its support.

NOMENCLATURE

a	=	surface area per unit volume[m ⁻¹]
c_p	=	specific heat of the fluid[Jkg ⁻¹ K ⁻¹]
D_{km}	=	binary diffusion coefficient [Jkg ⁻¹ K ⁻¹]
d_p	=	particle diameter[m]
H	=	volumetric heat transfer coefficient, ah_c [Wm ⁻³ K ⁻¹]
h	=	Enthalpy [J kg ⁻¹]
h_c	=	heat transfer coefficient[W m ⁻² K ⁻¹]
I	=	radiant intensity [W m ⁻² sr ⁻¹]
N_T	=	number of particles per unit volume [m ⁻³]
N_u	=	Nuselt number [-]
p	=	Pressure[N m ⁻²]
q	=	radiant heat flux [W m ⁻²]
Re	=	Reynolds number, $\rho\rho U d_p \mu^{-1}$
$R_{contact}$	=	thermal contact resistance [m ² K W ⁻¹]
R_t	=	total contact resistance [m ² K W ⁻¹]
r	=	radial coordination [m]
s	=	Radiative geometry path length [m]
\hat{S}	=	unit vector into a given direction[-]
T	=	temperature [K]
u	=	axial velocity [m s ⁻¹]
v	=	radial velocity [m s ⁻¹]
W_k	=	Molecular weight of species k [kg kmole ⁻¹]
x	=	axial coordination [m]
Y_k	=	mass fraction of species k [-]

Greek Symbols

$\Delta P / \Delta L$	=	pressure loss along ΔL due to the porous matrix [N m ⁻³]
β	=	extinction coefficient [m ⁻¹]
ϕ	=	Porosity [-]
Φ	=	scattering phase function [sr ⁻¹]
κ	=	absorption coefficient [m ⁻¹]
μ	=	viscosity [W m ⁻¹ K ⁻¹]
ρ	=	density [kg m ⁻³] or reflectivity [-]
α	=	absorptivity [-]
σ_s	=	scattering coefficient [m-1]
Ω	=	solid angle [sr]
ω	=	scattering albedo [-]
$\dot{\omega}_k$	=	molar rate of reaction of species k [kmole m ⁻³ s ⁻¹]
λ	=	thermal conductivity [Wm ⁻¹ K ⁻¹]
σ	=	Stephan-Boltzman constant [5.670 × 10 ⁻⁸ W m ⁻² K ⁴]
ϵ	=	emissivity [-]

Subscripts

b	blackbody
c	coolant
f	fluid
r	radiation
s	solid
η	at a given wavenumber

REFERENCES

[1] F. J. Weinberg, Combustion temperatures: the future? Nature 1971;233:239-41

[2] T. Takeno, K. Sato, K. Hase. "A theoretical study on an excess enthalpy flame". In: *Proceedings of the 18th Symposium (International) on Combustion*, Waterloo, 1981. pp. 465-72.

[3] D.K. Min and H.D. Shin "Laminar Premixed Flame Stabilization inside a Honeycomb Ceramic", *Int. J. Heat Mass Transfer*, vol. 34, 1991, pp. 341-356.

[4] V. Khanna, R. Goel and J.L. Ellzey, "Measurements of Emissions and Radiation for Methane Combustion with in a Porous Medium Burner," *Combustion science and Technology*, vol. 99, 1994, pp. 133-142

[5] D. Trimis, F. Durst, "Combustion in a porous medium—advances and applications," *Combustion science and Technology*, vol. 121, 1996, pp. 135-168

[6] J.R. Howell, H.J. Hall and J.I. Ellzey, "Combustion of Hydrocarbon

Fuels Within Porous Inert Media" *Prog. Energy Combust. Sci.* vol. 22, 1996, pp. 121-145

[7] P. F. Hsu, J. R. Howell, and R. D. Matthews, *Proceeding of the ASME/JSME Thermal Engineering Joint Conference*, vol. 4, 1991, pp. 225-231.

[8] Zhou X.Y. and Pereira J.C.F. "Numerical Study of Combustion and Pollutions Formation in inert Non homogenous Porous Media," *Combustion science and Technology*, vol. 130, 1997, pp. 335-364.

[9] D.J. Diamantis, E. Mastorakos, and D.A. Goussis, "Simulations of Premixed Combustion in Porous Media," *Combustion Theory Modelling*, vol. 6,202, pp. 383-411.

[10] M. T. Smucker and J.L. Ellzey, "Computational and Experimental Study of A two-Section Porous Burner," *Combustion science and Technology*, vol. 176, 2004, pp. 1171-1189.

[11] F. Durst and D. Trimis, "Compact low emission combustion reactors with integrated heat exchangers using porous medium combustion," *First European Conference on Small Burner Technology and Heating equipment*, vol. 1, 25-26 September 1996, Zurich, Switzerland, 1997(a)

[12] D. G. Nicol, P. C. Malte, "Development of a Five step Global Methane Oxidation-NO Formation Mechanism for lean Premixed Gas Turbine Combustion," *Journal of Engineering for Gas Turbines and Power* (Transaction of the ASME), vol. 121, 1999, pp. 272-280.

[13] N. Wakao and S. Kagueli, *Heat and Mass Transfer in Packed Beds*. London: Gordon and Breach Science Publisher, 1982.

[14] L.B. Younis and R. Viskanta, "Experimental determination of the volumetric heat transfer coefficient between stream of air and ceramic foam," *Int. J. Heat Mass Transfer*, vol. 36, 1993, pp. 1425-1434.

[15] I. F. Macdonald, M. S. El-Sayed, K. Mow, and F. A. L. Dullien, "Flow through porous media Ergun equation revisited," *Ind. Eng. Chem. Fund.*, vol. 18, 1979, pp.199-208.

[16] P. F. Hsu and J. R. Howell, "Measurements of thermal conductivity and optical properties of porous partially stabilized zirconia," *Experimental Heat Transfer*, vol. 5, 1993, pp. 293-313.

[17] M. F. Modest, *Radiative Heat Transfer*. New York: McGraw-Hill, 1993

[18] S.V. Patankar , D.B. Spalding, "A Calculation Procedure for Heat, Mass and Momentum Transfer in Three-Dimensional Parabolic Flows," *Int. J. Heat Mass Trans.* vol. 15, 1972, pp.1787-1806.

[19] J. C. Chai, H. S. Lee, S. Patankar, "Finite Volume Method for Radiation Heat Transfer," *Journal of Thermophysics and Heat Transfer*, vol. 8, No. 3, 1994, pp. 419-425.

[20] F. Durst and D. Trimis, *Compact Porous Medium Burner and Heat Exchanger for Household Applications, EC project report (contract no. JOE3-CT95-0019)*, 1996